Upregulation of RNase E activity by mutation of a site that uncompetitively interferes with RNA binding

Hayoung Go, Christopher J. Moore, Minho Lee, Eunkyoung Shin, Che Ok Jeon, Chang-Jun Cha, Seung Hyun Han, Su-Jin Kim, Sang-Won Lee, Younghoon Lee, Nam-Chul Ha, Yong-Hak Kim, Stanley N. Cohen & Kangseok Lee

Upregulation of RNase E activity by mutation of a site that uncompetitively interferes with RNA binding

Hayoung Go,[1,2,†] Christopher J. Moore,[2,†] Minho Lee,[1] Eunkyoung Shin,[1] Che Ok Jeon,[1] Chang-Jun Cha,[1] Seung Hyun Han,[3] Su-Jin Kim,[4] Sang-Won Lee,[4] Younghoon Lee,[5] Nam-Chul Ha,[6] Yong-Hak Kim,[7,*] Stanley N. Cohen[2,8,*] and Kangseok Lee[1,*]

[1]School of Biological Sciences; Chung-Ang University; Seoul, Republic of Korea; [2]Department of Genetics; Stanford University; Stanford, CA USA; [3]Department of Oral Microbiology and Immunology; Seoul National University; Seoul, Republic of Korea; [4]Department of Chemistry; Korea University; Seoul, Republic of Korea; [5]Department of Chemistry; KAIST; Daejeon, Republic of Korea; [6]Department of Manufacturing Pharmacy; Pusan National University; Busan, Republic of Korea [7]Department of Microbiology; Catholic University of Daegu; Daegu, Republic of Korea; [8]Department of Medicine; Stanford University; Stanford, CA USA

[†]These authors contributed equally to this work.

Escherichia coli RNase E contains a site that selectively binds to RNAs containing 5′-monophosphate termini, increasing the efficiency of endonucleolytic cleavage of these RNAs. Random mutagenesis of N-Rne, the N-terminal catalytic region of RNase E, identified a hyperactive variant that remains preferentially responsive to phosphorylation at 5′ termini. Biochemical analyses showed that the mutation (Q36R), which replaces glutamine with arginine at a position distant from the catalytic site, increases formation of stable RNA-protein complexes without detectably affecting the enzyme's secondary or tertiary structure. Studies of cleavage of fluorogenic substrate and EMSA experiments indicated that the Q36R mutation increases catalytic activity and RNA binding. However, UV crosslinking and mass spectrometry studies suggested that the mutant enzyme lacks an RNA binding site present in its wild-type counterpart. Two substrate-bound tryptic peptides, [65]HGFLPLK[71]—which includes amino acids previously implicated in substrate binding and catalysis— and [24]LYDLDIESPGHEQK[37]—which includes the Q36 locus—were identified in wild-type enzyme complexes, whereas only the shorter peptide was observed for complexes containing Q36R. Our results identify a novel RNase E locus that disparately affects the number of substrate binding sites and catalytic activity of the enzyme. We propose a model that may account for these surprising effects.

Introduction

The degradation and processing of RNAs in bacterial cells involves numerous *cis*- and *trans*-acting agents. Among these, RNase E (Rne), an endoribonuclease, has been shown to play a key enzymatic role in *Escherichia coli*. The essential 118 kDa Rne protein contains 1,061 amino acids that can be grouped into three functionally distinct domains. The catalytic function and cleavage site specificity of RNase E reside in the N-terminal part of the protein (amino acid residues 1 to 498),[1] which is sufficient for cell survival.[2,3] A smaller RNase E derivative that contains the first 395 amino acid residues retains certain enzymatic activities, whereas further truncation leads to their loss.[4] The X-ray crystal structure of the N-terminal half of RNase E (amino acid residues 1 to 529) revealed several sub-domains: an RNase H-like domain, the RNA-binding S1 region, a 5' sensor pocket, a DNase I-like domain, the Zn^{2+}-linking region, and a "small domain" that mediates multimer formation.[5,6] The arginine-rich domain located between amino acids 580 and 700 plays a role in RNA-binding.[7] The C-terminal third of the RNase E protein serves as a platform for the formation of a multi-component 'degradosome' complex (for a recent review, see ref. 8).

X-ray crystallography has revealed that the N-terminal part of RNase E forms a quaternary structure comprised of a dimer of dimers connected via their small domains (amino acid residues 416–529). It has been reported that 5'-end dependent RNA cleavage by RNase E requires the formation of protein multimers[9] and that alterations of the binding motif that abolish multimer formation substantially reduce RNase E catalytic activity.[10] However, Caruthers et al.[4] found that RNase E derivatives that

lack the Zn-link and small domains essential for dimer and tetramer formation still retain cleavage activity—albeit much reduced—as well as substrate specificity, and can support the survival of *rne* null mutant *E. coli*. Recent studies have shown that aside from its enzymatic functions, RNase E also acts as a cytoskeletal protein,[11] which was previously suspected based on the observation that RNase E cross-reacted with antibodies raised against the yeast myosin heavy chain.[12]

RNase E cleaves A-U rich, single-stranded regions within substrate RNA (for reviews see refs. 13–15). The cleavage rate and substrate binding of RNase E are profoundly influenced by the state of 5'-phosphorylation of substrates.[9,16,17] Study of X-ray crystal structures of the N-terminal part of RNase E complexed to short synthetic oligonucleotide substrates has resulted in a model that accounts for the preference of RNase E for RNA substrates having a 5'-monophosphate group.[5,18] The discovery that a pyrophosphatase called RppH accelerates transcript degradation has demonstrated the physiological importance of the 5' end in RNase E-mediated cleavages.[19,20] Investigations of the effects of 2'-O-methyl nucleotide substitutions in RNA substrates on the ability of those substrates to be cleaved by RNase E have suggested that the RNase E catalytic region makes contact with at least two separate locations in substrates,[17] and a recent study that reported rapid RNase E cleavage of RNA lacking a 5'-monophosphate stimulation[21] also supports the notion that there is more than one point of contact between RNase E and its substrates.[13]

While characterizing an RNase E mutation that leads to hyperactivity of the enzyme, we found that this mutation, which results in a glutamine to arginine substitution at position 36, also enhances the ability of RNase E to bind to RNA substrates, but reduces the apparent number of RNA binding sites based on RNA-protein as determined by crosslinking analysis. Dissociation of the number of substrate binding sites from the overall binding affinity and catalytic activities of the enzyme by this point mutation suggests a model in which interaction between enzyme and substrate at a hitherto cryptic locus may negatively regulate catalysis in the wild-type protein.

Results

Isolation of hyperactive N-Rne mutants. To isolate hyperactive RNase E mutants, we used a genetic approach analogous to that used to screen for loss-of-function mutants of RNase E;[22] here, we introduced random mutations in the coding region of the minimal catalytic domain of Rne in pNRNE4. The DNA segment encoding amino acids 1-398 of Rne was amplified using error-prone PCR, ligated into pNRNE4 by replacing the corresponding wild-type segment of *N-rne*, and the resulting ligation product was introduced by transformation into *E. coli* strain KSL2000.[23] KSL2000 has a chromosomal deletion in *rne* that is complemented by a plasmid-born *rne* gene under the control of an arabinose-inducible promoter (pBAD-RNE). Whereas KSL2000 cells are unable to grow in the absence of arabinose,[23,24] addition of 0.2% arabinose to cultures of KSL2000 induces the synthesis of full-length RNase E at wild-type levels, and consequently supports survival and growth of the *rne* deletion mutant.

pNRNE4, a compatible plasmid bearing an ampicillin resistance (Ap^r) marker, expresses the N-terminal 498 amino acids of RNase E fused to a hexahistidine tag at the C-terminus (N-Rne) under control of the isopropyl-β-D-thiogalactopyranoside (IPTG)-inducible *lacUV5* promoter; KSL2000 cells harboring pNRNE4 are able to grow normally in the presence of 10-100 μM IPTG, even when cultured without arabinose (**Fig. 1A**). In these experiments, autoregulation of RNase E was circumvented by expressing N-Rne and Rne from an *N-rne* and an *rne* gene lacking the 5'-UTR, respectively.

Transformants were tested individually for their ability to support the growth of KSL2000 cells on LB-agar medium containing 1-1,000 μM IPTG but lacking arabinose. A total of ~5,000 transformants were tested, and we obtained two clones that grew normally in the presence of 1-10 μM IPTG but which in media containing 100-1,000 μM IPTG showed a decreased rate of growth compared to cells expressing wild-type N-Rne (**Fig. 1A**). Because the detrimental effects of excessive RNase E activity on cell viability were observed at a lower level of IPTG induction, we tentatively designated these clones as hyperactive RNase E mutants. Sequencing analysis revealed that both bacterial clones we obtained had a single amino acid substitution: one substitution was in the S1 domain (Q36R; glutamine to arginine) while the other was located in the RNase H domain (V236E; valine to glutamic acid). Both of these amino acids are situated on a surface distant from the catalytic site and the partner protomer of the dimer according to the crystal structure of the N-terminal part of RNase E[5] (**Fig. 1B**). As the V236E mutation less severely affected cell growth when overexpressed (**Fig. 1A**) and resulted in less of an increase in ribonucleolytic cleavage activity in vitro (data not shown), we chose the Q36R mutation for further analyses.

Effects of the Q36R substitution on the cleavage activity of N-Rne in vivo. To determine whether the ability of the N-Rne mutant (N-Rne-Q36R) to support cell viability at lower levels of IPTG-induced expression than wild-type N-Rne (N-Rne-wt) resulted from an increase in ribonucleolytic activity, we analyzed the steady-state level of RNA I in KSL2000 cells conditionally expressing N-Rne-Q36R in the absence of full-length RNase E. RNase E cleaves RNA I, which is an antisense regulator of ColE1-type plasmid DNA replication;[25] this function has been used to assess the ribonucleolytic activity of RNase E in vivo by measuring ColE1-type plasmid copy number relative to an RNase E independent plasmid.[22,26,27]

Transiently induced expression of the N-Rne-Q36R mutant by 100 μM IPTG resulted in an approximately 2.6-fold greater copy number of the pNRNE4-Q36R plasmid than was observed in KSL2000 cells containing the similarly induced wild-type N-Rne (**Fig. 2A**). Full-length RNase E was not detected by western blot analysis. The abundance of N-Rne-Q36R protein in KSL2000 cells was higher than was observed for wild-type N-Rne, consistent with the increased copy number of the pNRNE4-Q36R plasmid relative to the pNRNE4 plasmid expressing the corresponding wild-type enzyme (**Fig. 2B**). However, the increase in enzyme abundance was less than the increase in plasmid copy number. We confirmed that the increased plasmid copy number results from more rapid degradation of RNA I in these cells by
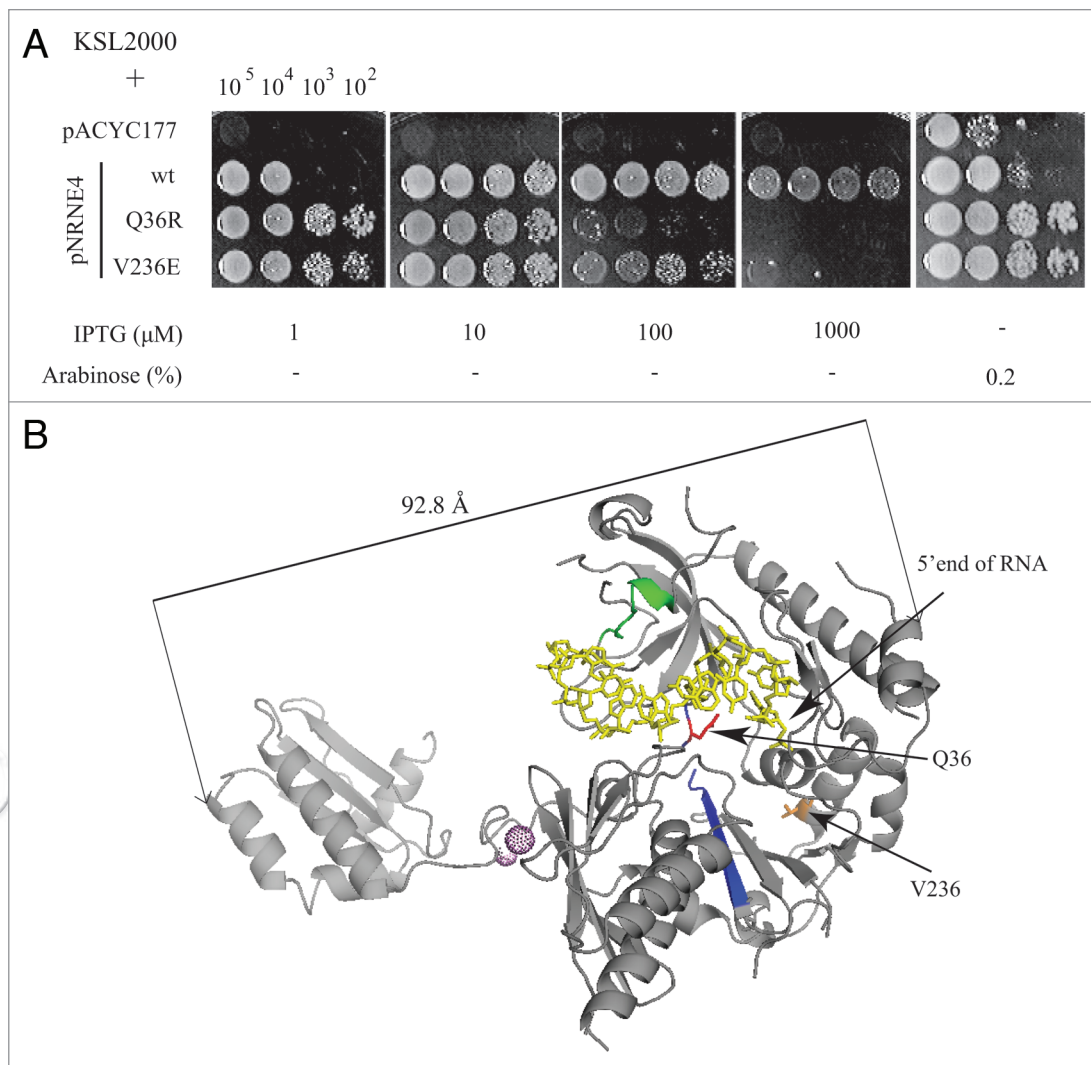
Figure 1. Identification of hyperactive N-Rne mutants. (A) Growth characteristics of cells expressing N-Rne mutants. KSL2000 cells harboring pNRNE4, pNRNE4-Q36R, or pNRNE4-V236E were evaluated individually on LB-agar plates containing 1-1000 μM of IPTG for their ability to support the growth of KSL2000 cells. KSL2000 containing pACYC177 grew only when full-length RNase E was expressed from pBAD-RNE in the presence of 0.2% arabinose. Numbers on the top indicate number of bacterial cells in each spot. (B) Locations of the isolated single amino-acid substitutions in the crystal structure of the N-terminal part of RNase E.[5] Two tryptic peptides that were UV crosslinked to a uridine base of p-BR13, [24]LYDLDIESPGHEQK[37] and [65]HGFLPLK[71] are colored in blue and green, respectively. p-BR13 is colored in yellow. The diagram was generated using PyMOL software.

direct measurement of decay rates using Northern blot analyses (**Fig. 2C**). The half-life of RNA I decreased from ~4.5 min in KSL2000 cells expressing IPTG-induced wild-type N-Rne to ~1.8 min in KSL2000 cells expressing similarly induced N-Rne-Q36R. However, the steady-state level of RNA I (i.e., the RNA I abundance at 0 min, prior to the addition of rifampicin) in KSL2000 cells that express N-Rne-Q36R was approximately 2.5 fold higher than in KSL2000 cells expressing N-Rne-wt, which also reflected an elevation of RNA I production due to the effects of the hyperactive enzyme on the copy number of pNRNE4-Q36R plasmid (**Fig. 2A**). The observed changes in plasmid copy number correlate with an increase in RNase E activity on RNA I.

The conclusion that the hyperactive phenotype of N-Rne-Q36R results from enhanced ribonucleolytic activity was confirmed by measuring the half-life of another RNase E substrate,

rpsT mRNA encoding ribosomal protein S20.[28] The half-life of *rpsT* mRNA transcribed from P1 and P2 promoters in KSL2000 cells expressing wild-type N-Rne decreased from ~1.3 and ~2.0 min to ~0.7 and ~0.6 min, respectively, in KSL2000 cells expressing N-Rne-Q36R (**Fig. 2D**), further showing that the Q36R mutation increases RNA cleavage activity in vivo.

Effects of the Q36R substitution on the ribonucleolytic activity of full length Rne in vivo. We wished to know whether the hyperactive phenotype conferred by a single amino acid substitution in N-Rne is maintained in the full length Rne protein. The Q36R mutation was introduced into a plasmid expressing full-length RNase E under the control of the IPTG-inducible *lacUV5* promoter (pLAC-RNE2), and the resulting plasmid (pLAC-RNE2-Q36R) was introduced into KSL2000 cells. Because the pLAC-RNE2 plasmid has the same replication
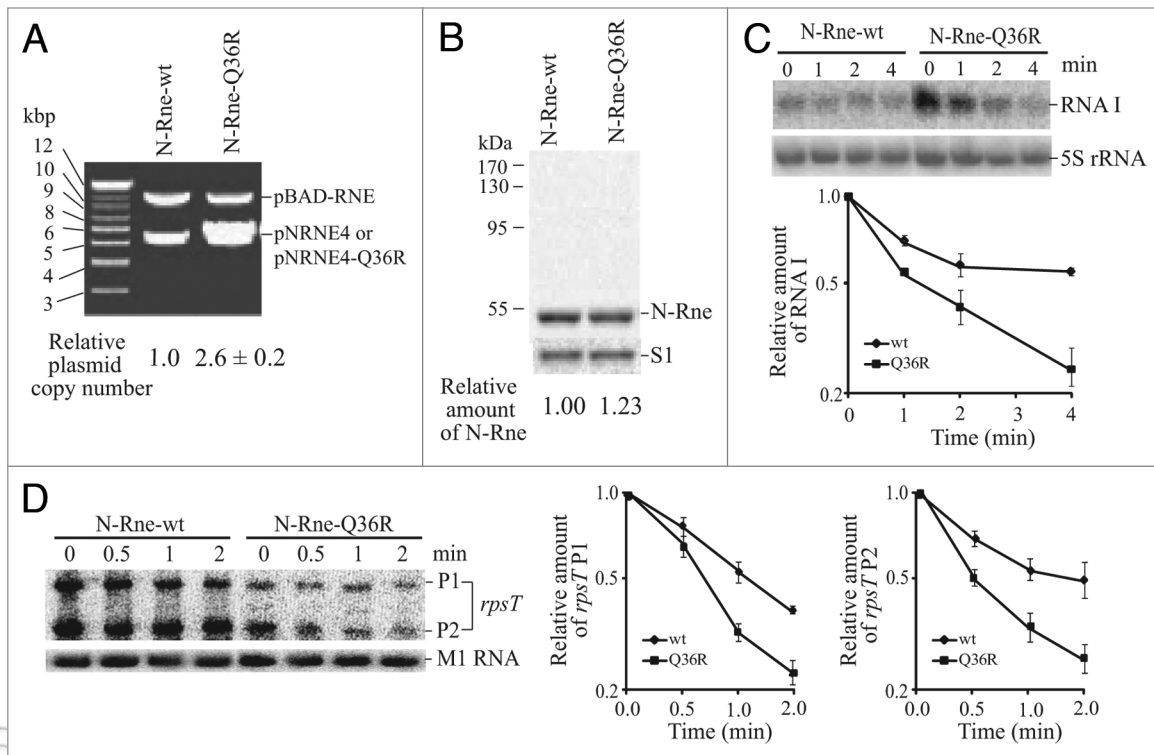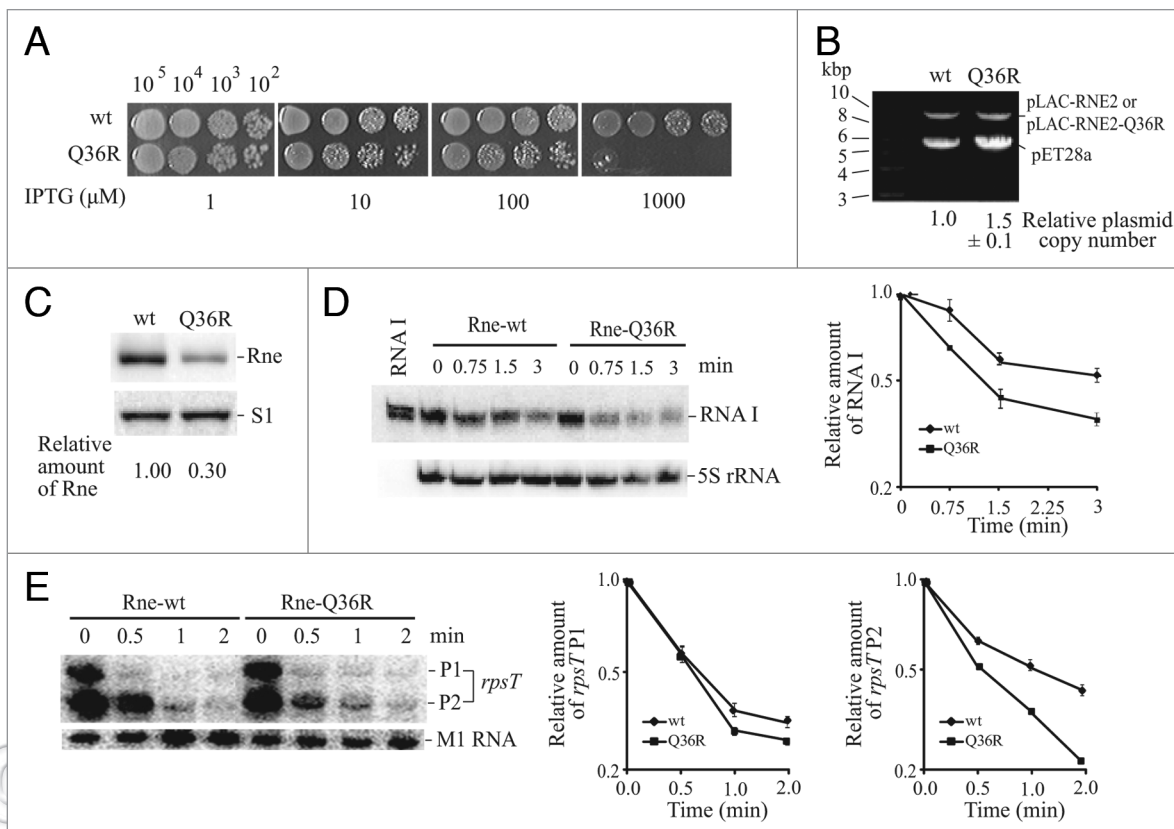
Figure 2. Effects of Q36R on the ribonucleolytic activity of N-Rne in vivo. (A) Plasmid copy number of pNRNE4 in KSL2000. Plasmids were purified from KSL2000 cells harboring pNRNE4 or pNRNE4-Q36R, and digested with HindIII, which has a unique cleavage site in all plasmids tested here. Plasmid copy numbers were calculated relative to a concurrently present pSC101 derivative (pBAD-RNE), the replication of which is independent of Rne, by measuring the molar ratio of ColE1-type plasmid (pNRNE4 and pNRNE4-Q36R) to the pBAD-RNE plasmid, and are shown at the bottom of the gel. (B) Expression profiles of N-Rne and mutant N-Rne proteins in KSL2000. The membrane probed with an anti-Rne monoclonal antibody was stripped and reprobed with an anti-S1 polyclonal antibody to provide an internal standard. The relative abundance of protein bands was quantified by setting the amount of N-Rne-wt to 1. (C) Half-life of RNA I in KSL2000 harboring pNRNE4 or pNRNE4-Q36R. Total RNA was prepared from the cultures taken before (0 min) and after addition of rifampicin (1 mg/ml) at time intervals indicated. The same membrane probed for RNA I of pACYC 177-derived plasmids was stripped and probed for 5S rRNA, which served to normalize the radioactivity present in the RNA I band in each lane. (D) Half-life of *rpsT* mRNA in KSL2000 harboring pNRNE4 or pNRNE4-Q36R. Total RNA was prepared from the cultures taken before (0 min) and after addition of rifampicin (1 mg/ml) at time intervals indicated. The same membrane probed for *rpsT* mRNA was stripped and probed for M1 RNA, which served to normalize the radioactivity present in the *rpsT* mRNA band in each lane. The relative abundance of RNA I or *rpsT* mRNA bands was quantified by phosphorimaging, setting the amount of RNA I or *rpsT* mRNA at 0 min to 1, and plotted in the graph. *rpsT* mRNA transcribed from P1 and P2 promoters are indicated as P1 and P2. The Northern blot experiments were repeated three times and averaged. The error bars (standard errors of the mean) were used to indicate the range of assay results. The half-life of RNA I in KSL2000 cells expressing wild-type N-Rne was estimated by fitting and extrapolating the plot in 2C.

origin as pBAD-RNE, which is derived from pSC101, but a different antibiotic resistance marker (Ap^r), we were able to construct a strain (KSL2003-Q36R) that expresses only the mutant RNase E protein (Rne-Q36R) by using a plasmid displacement procedure.[23] The same method had been previously used to create the strain KSL2003, which harbors the pLAC-RNE2 plasmid and expresses the wild type version of RNase E. As in the previous experiments, autoregulation of RNase E was circumvented by expressing RNase E from an *rne* gene lacking the 5'-UTR that was placed downstream from the IPTG-inducible *lacUV5* promoter in plasmid pLAC-RNE2.

Transformants were grown for 60-80 generations in the presence of 10 μM IPTG and ampicillin (50 μg/ml), and replacement of the resident plasmid (pBAD-RNE) in KSL2000 with the incoming plasmid (pLAC-RNE2-Q36R) was confirmed by testing the cells for sensitivity to kanamycin, which is an antibiotic marker for pBAD-RNE. This procedure has been successfully used to test the ability of RNase E homologs to functionally complement RNase E in *E. coli*.[23,24,26] The resulting strain (KSL2003-Q36R) was more sensitive to high concentrations of IPTG than KSL2003, indicating that the effect of this amino acid substitution is not specific to the truncated form of RNase E, N-Rne (**Fig. 3A**).

Additional evidence of the ability of the mutant RNase E protein to cleave RNA I more efficiently than wild-type RNase E does was obtained by introducing a ColE1-type test plasmid (pET28a) into KSL2003-Q36R cells and measuring the copy number of pET28a relative to that of the pLAC-RNE2-derived plasmid. Although western blotting indicated that the abundance of the full length Rne-Q36R protein was reduced to ~30% of the wild-type level (**Fig. 3C**), cells expressing Rne-Q36R showed an approximately 1.5-fold increase in the copy number of pET28a relative to that observed in cells expressing wild-type Rne (**Fig. 3B**). Taken together, these findings suggest that an Rne protein bearing

Figure 3. Effects of Q36R on the ribonucleolytic activity of Rne in vivo. (A) Growth characteristics of KSL2003 cells expressing Rne and Rne-Q36R. KSL2003 cells harboring pLAC-RNE2 or pLAC-RNE2-Q36R were evaluated individually on LB-agar plates containing 1-1000 µM of IPTG for their ability to support the growth of KSL2003 cells. Numbers on the top indicate number of bacterial cells in each spot. (B) Plasmid copy number of pET28a in KSL2003. Plasmids were purified from KSL2003 or KSL2003-Q36R cells harboring pET28a and digested with HindIII, which has a unique cleavage site in all plasmids tested here. Plasmid copy numbers were calculated relative to concurrently present pSC101 derivatives (pLAC-RNE2 or pLAC-RNE2-Q36R) as described in the legend to **Fig. 2A**. (C) Expression profiles of Rne and mutant Rne proteins in KSL2003. The same procedure described in the legend to **Fig. 2B** was used for western blot analysis. KSL2003 and KSL2003-Q36R cells were grown in LB media containing 10 µM of IPTG. (D) Half-life of RNA I in KSL2003 and KSL2003-Q36R. (E) Half-life of *rpsT* mRNA in KSL2003 and KSL2003-Q36R. The same procedure described in the legend to **Fig. 2C** and **Fig. 2D** was used for northern blot analysis of RNA I of pBR322-derived plasmids and *rpsT* mRNA. Ten nanograms of in vitro synthesized RNA I of pBR322 was loaded in the first lane of the gel in **Fig. 3D**.

Q36R is less stable than the wild-type protein but much more active in cleaving RNA I.

We confirmed that the increased plasmid copy number results from more rapid decay of RNA I in the KSL2003-Q36R strain by using Northern blot analyses (**Fig. 3D**). Whereas the steady-state level of RNA I in KSL2003-Q36R cells was not significantly altered, again because enhanced decay of RNA I leads to an increased copy number of the ColE1-type plasmid and consequently increased dosage of the plasmid-borne Rne gene, (**Fig. 3D**), the half-life of RNA I decreased from ~3.0 min in KSL2003 cells expressing wild-type Rne to ~1.2 min in KSL2003 cells expressing Rne-Q36R. We obtained analogous results from the measurement of half-life of *rpsT* mRNA. The half-life of *rpsT* mRNA transcribed from the P2 promoter in KSL2003 cells expressing wild-type Rne decreased by 50% (from ~1.0 to ~0.5) in KSL2003 cells expressing Rne-Q36R. The half-life of *rpsT* mRNA transcribed from the P1 promoter was not significantly changed, probably due to its relatively high instability in *E. coli* cells expressing full-length RNase E (**Fig. 3E**). Taken

together, these results demonstrate the enhanced in vivo RNA cleavage activity of the hyperactive Rne mutant and that the effects of the Q36R mutation are not restricted to N-Rne in vivo.

Cross-linking and CD analysis of N-Rne-Q36R. Purified protein preparations from KSL2000 cells that conditionally over-expressed wild-type N-Rne (N-Rne-wt) or N-Rne-Q36R in the absence of RNase E expression (no arabinose) did not contain detectable amounts of other proteins (**Fig. 4A**). These proteins were found to have a similar circular dichroism (CD) profile, indicating that the Q36R mutation does not significantly change the secondary or tertiary structure of the enzyme (**Fig. 4B**). We also tested the ability of the Q36R mutant protein to form multimers using UV crosslinking. As shown in **Fig. 4C**, N-Rne-Q36R formed multimers to a similar degree as N-Rne-wt.

In vitro RNA cleavage activity of N-Rne-Q36R. Affinity-purified wild-type and N-Rne-Q36R proteins were tested for their ability to cleave RNase E substrates in vitro under single-turnover conditions. First, we measured the rates of in vitro cleavage by the wild-type and N-Rne-Q36R proteins on BR13, an
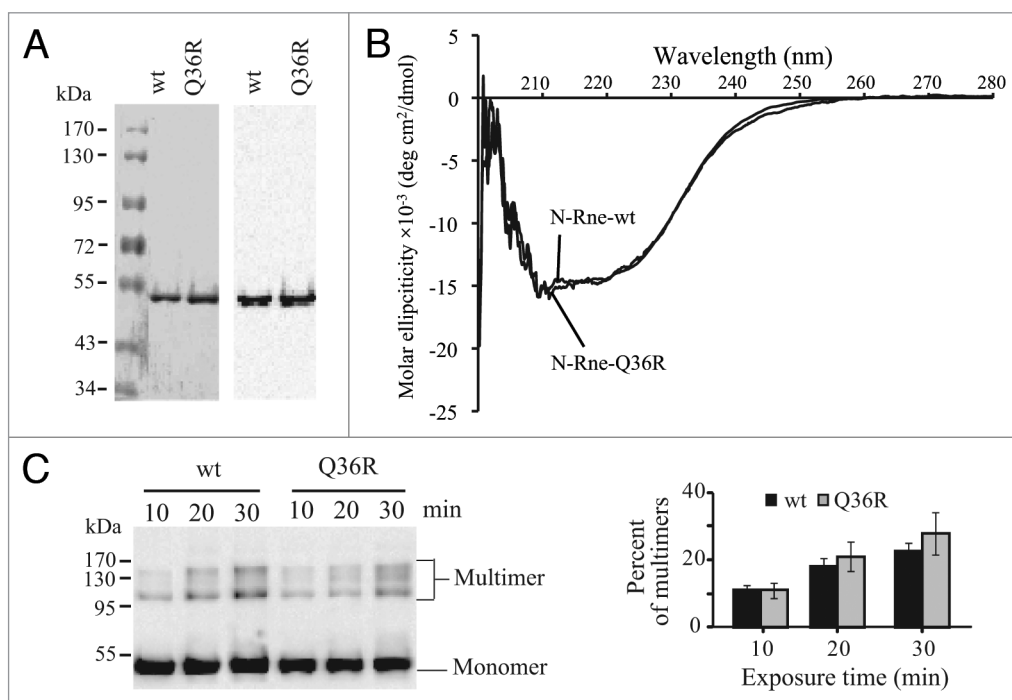
Figure 4. Properties of affinity purified N-Rne-Q36R. (A) Coomassie blue stain and western blot analyses of affinity-purified wild-type N-Rne and N-Rne-Q36R. Purified N-Rne-wt and N-Rne-Q36R western blot using an anti-Rne monoclonal antibody (right panel). (B) Structural integrity of the N-Rne-Q36R. Purified proteins were used to measure the CD spectrum. The overall spectrum of the protein was similar to that of lysozyme, which has a secondary structure content comparable to N-Rne. The secondary structure content of the protein, which was analyzed by the program K2D2,[42] showed a result compatible with the expected values. (C) Effects of Q36R on multimer formation of N-Rne. Purified proteins were UV crosslinked at various time intervals, separated by SDS-PAGE, and immunoblotted using an anti-Rne monoclonal antibody (left panel). Percent of multimers were quantified and shown in the right panel.

oligoribonucleotide that contains the RNase E targeted cleavage site of RNA I. Purified N-Rne-wt or N-Rne-Q36R proteins were incubated with the 5'-triphosphorylated substrate ppp-BR13, which was uniformly labeled with $[\alpha\text{-}^{32}\text{P}]$-UTP and the cleavage products were analyzed by PAGE. The N-Rne-Q36R protein cleaved ppp-BR13 faster than the wild-type N-Rne did (**Fig. 5A**); during an initial 30 min period following addition of enzyme, the rate of ppp-BR13 cleavage by N-Rne-Q36R was ~3.0 times greater than was observed for N-Rne-wt. A corresponding increase in the rate of cleavage was observed for 5'-end-labeled BR13 containing a monophosphate at the 5'-end (p-BR13) (**Fig. 5B**). The rate of cleavage by N-Rne-Q36R during the first min following addition of the enzyme was ~2.5-fold higher than for N-Rne-wt, while the cleavage rates for the later times were largely similar (**Fig. 5B**). However, notwithstanding the ability of the Q36R mutation to increase the rate of cleavage on both ppp-BR13 and p-BR13, the hyperactive mutant enzyme retained the ability to distinguish between 5'-monophosphorylated RNA and 5'-triphosphorylated RNA, continuing to cleave the former more rapidly than the latter (**Fig. 5A and Fig. 5B**). The hyperactivity of the N-Rne-Q36R mutant enzyme was also evident in cleavage of p23, a truncated pM1-derived RNA that is processed by RNase E to a product termed 23 RNA.[29] N-Rne-Q36R cleaved synthetic p23 RNA at a rate ~3.0-fold higher than was seen for wild-type N-Rne, and the rate of cleavage of p23 RNA by N-Rne-Q36R remained similar throughout the reaction (**Fig. 5C**). These results indicate that the

increased cleavage activity of N-Rne-Q36R is not restricted to the RNase E-targeted sequence of RNA I.

It has been shown that 3' to 5' directionality in cleavage site selection is an inherent property of RNase E catalysis.[4] We tested whether this property of RNase E is altered by the Q36R mutation via an in vitro cleavage assay using BR30, an oligonucleotide containing three repeats of a target sequence of BR13.[17] As shown in **Fig. 5D**, N-Rne-Q36R exhibited 3' to 5' directionality in cleavage site selection similar to that of N-Rne-wt. The N-Rne-Q36R mutant enzyme was also able to more efficiently cleave BR30 without changing cleavage site specificity.

Analyses of binding and cleavage activities of N-Rne-wt and N-Rne-Q36R proteins. We measured the RNA binding capability of N-Rne-Q36R using an electrophoretic mobility shift assay (EMSA). The RNA dissociation constants (K_D) of N-Rne-Q36R to ppp-BR13 and p-BR13 were decreased by approximately two-fold compared to those of N-Rne-wt (40.5 versus 85.65 µM for ppp-BR13 and 8.96 versus 14.24 µM for p-BR13) (**Fig. 6A and Fig. 6B**), indicating that the mutant protein has a higher binding affinity for both substrates than its wild-type counterpart. However, notwithstanding the ability of the mutation to increase RNA binding to both 5'-monophosphorylated and 5'-triphosphorylated BR13, the N-RNE-Q36R protein still showed preferential binding to substrates having 5'-monophosphorylated termini, thus retaining this characteristic of the wild-type enzyme. The binding constants determined for N-Rne-Q36R
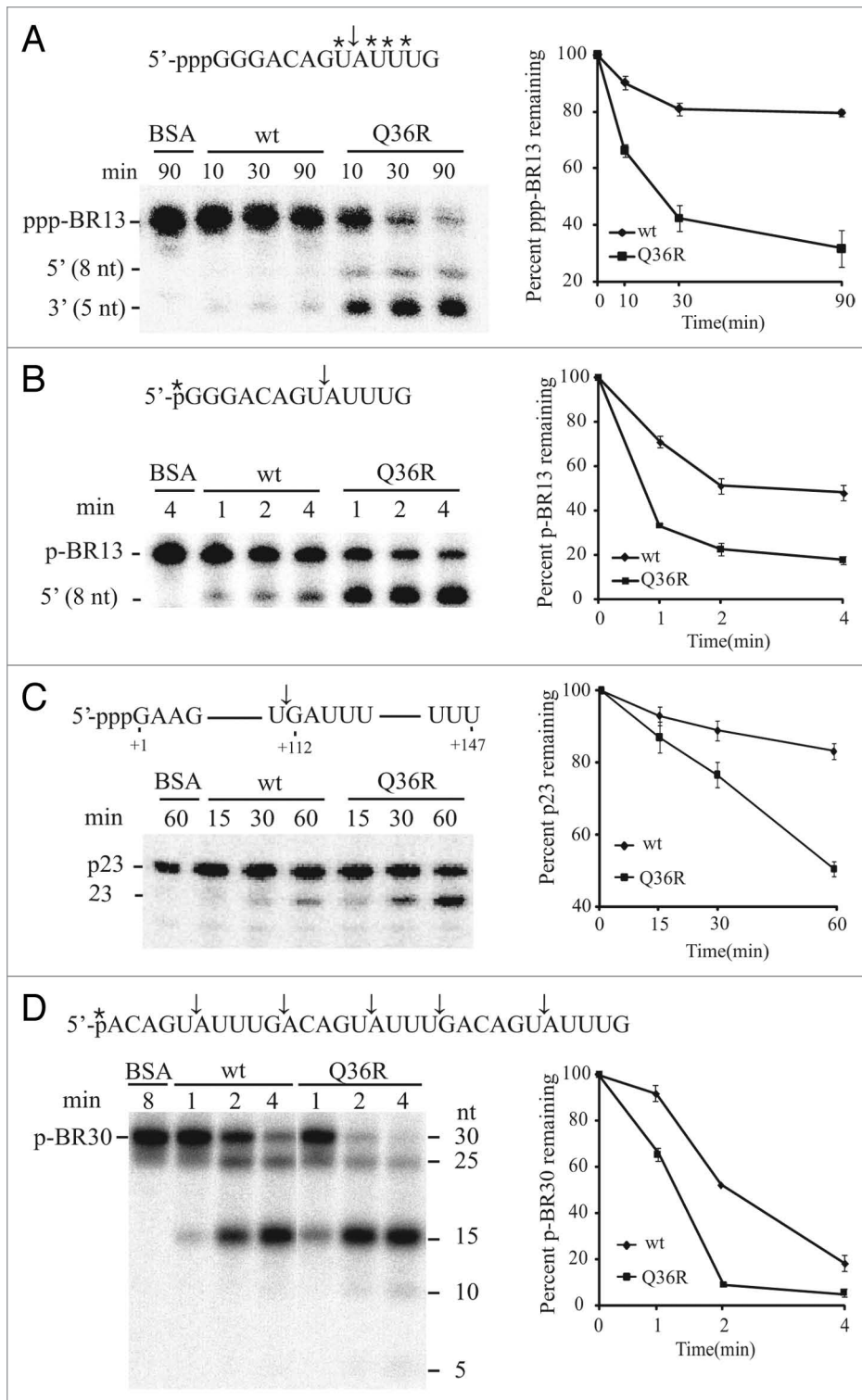
Figure 5. In vitro cleavage of RNase E substrates by N-Rne-wt and N-Rne–Q36R. Cleavage of 5′-triphosphorylated BR13 (ppp-BR13) (A), 5′-monophosphorylated BR13 (p-BR13) (B), 5′-triphosphorylated p23 RNA (C), and 5′-monophosphorylated BR30 (p-BR30) (D) by N-Rne-wt and N-Rne-Q36R. Half a picomole of RNA was incubated with one (for B and D) or 100 picomole (for A and C) of purified N-Rne-wt or N-Rne-Q36R in 100 μl of cleavage buffer at 37°C. The cleavage products of ppp-BR13 were undetectable when 0.5 pmol RNA and 1 pmol N-Rne were used in the reaction. Samples were removed at each time point indicated and mixed with an equal volume of loading buffer. Samples were denatured at 75°C for 5 min and loaded onto 8% (C) or 12% (A, B, and D) polyacrylamide gels containing 8 M urea. ppp-BR13 and p23 RNA were uniformly labeled with [α-^{32}P]-UTP. The radioactivity in each band was quantified using a phosphorimager and OptiQuant software. RNase E cleavage sites are indicated with arrows. The location of 32P-labeled phosphates in BR13 is indicated with asterisks.

does not affect the ability to sense and respond to the extent of phosphorylation at the substrate's 5′ terminus.

We examined whether the Q36R mutation renders N-Rne more catalytically active by measuring the Michaelis-Menten kinetic parameters k_{cat} and K_m for cleavage of fluorogenic P-BR14-FD.[9] The K_m value for the cleavage of this substrate by N-Rne-Q36R was two-fold higher (0.12 μM) than that of the wild-type N-Rne (0.06 μM), and the k_{cat} value of N-Rne-Q36R was also two-fold higher (13.30 min^{-1}) than that of N-Rne-wt (6.07 min^{-1}) (**Fig. 7**). These results suggest that N-Rne-wt may include an additional RNA binding site that reduces the enzyme's rate of activity by acting to inhibit the enzyme's catalytic site (see Discussion).
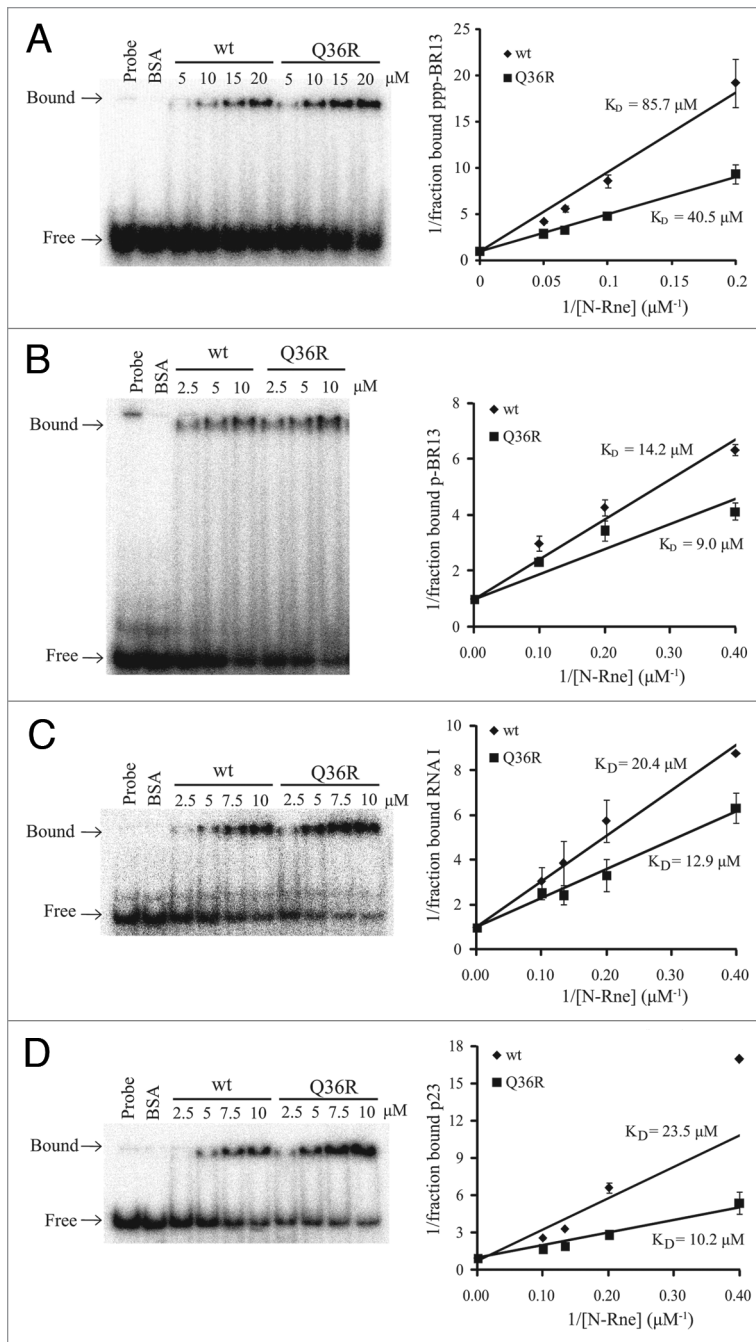
Identification of BR13 binding sites in N-Rne-wt and N-Rne-Q36R. The results presented above suggest that substrate RNAs make contact with N-Rne molecules at a site near the Q36

binding to the uniformly labeled, 5′-triphosphorylated transcripts RNA I and p23 RNA (12.90 and 10.18 μM, respectively) were similar to those observed using p-BR13 as substrate and reflected an approximately two-fold greater affinity than the wild-type N-Rne protein (**Fig. 6C and Fig. 6D**). These results argue that the Q36R mutation increases overall RNase E binding to both 5′-monophosphorylated and 5′-triphosphorylated substrates, but

locus, as well as at the previously identified, and physically distant, 5′ sensor site and S1 domain.[5] The existence of two points of contact between RNase E molecules and their substrates, including the S1 domain, was confirmed by UV-crosslinking studies using N-Rne and BR13. It has been shown that UV crosslinking at 254 nm generates a covalent bond between the side chains of UV-crosslinkable amino acids (methionine, tyrosine, histidine,
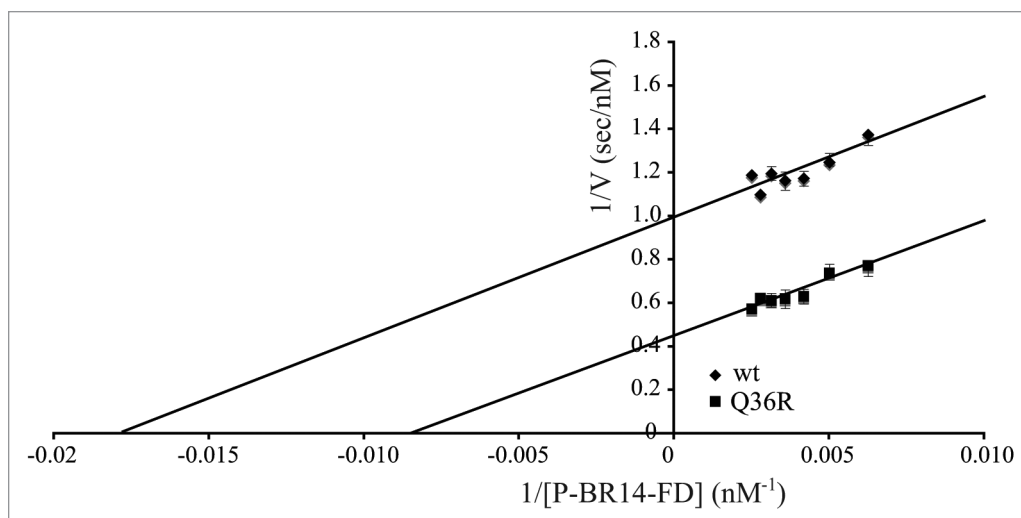
Figure 6. Effects of Q36R on the catalytic potency and RNA binding activity of N-Rne. One picomole of uniformly labeled ppp-BR13 (A), RNA I (C), or p23 RNA (D), or 5'-end labeled p-BR13 (B) was incubated with increasing concentrations of purified N-Rne-wt or N-Rne-Q36R proteins in 100 μl of an EMSA buffer and analyzed by 8% nondenaturing PAGE. Binding constants were calculated based on slopes calculated from the graphs in the right panel.

The specific regions of N-Rne proteins that bind to p-BR13 were identified by purifying proteins from UV-crosslinked reaction mixtures, digesting with trypsin, and analyzing the tryptic digests by mass spectrometry (MS). Results from reaction mixtures containing UV-crosslinked enzyme-RNA complexes, (lanes 2 and 5 in **Fig. 8A**), from mixtures containing non-UV-treated enzyme and pBR13 (lanes 3 and 6 in **Fig. 8A**), and mixtures containing enzyme that was irradiated by UV in the absence of BR13 (lanes 1 and 4 in **Fig. 8A**) were compared. Enzyme-pBR13 complexes were purified from the protein bands that consisted of protein monomers, treated in an alkaline buffer to hydrolyze the phosphodiester bonds of RNA, and digested with trypsin for MS analysis. The results obtained from mass spectrometric analyses of tryptic peptides derived from N-Rne-wt and N-Rne-Q36R covered 96.8% of the translated sequence, but excluded a short peptide region, [358]AVENR↓LR↓EAVR↓QDR[371], which is cleaved at the arrowed sites to produce only small peptides out of the detection range (<m/z 450) (**Supplementary Table S1**). The mass chromatograms showed highly reproducible peaks and charge distributions of the precursor ions within 10 ppm tolerance, and a peak derived from N-Rne-Q36R and containing the mutated [24]LYDLDIESPGHER[36] peptide was clearly distinguished from the wild-type [24]LYDLDIESPGHEQK[37]-containing peak seen in the N-Rne digest (**Fig. 8B**). As the groups most reactive to UV are a uridine base of RNA and the amino acid side chains of methionine, tyrosine, histidine, phenylalanine, leucine, and cysteine,[30,31] we judged the method employed to be adequate for identifying uridine-bound peptides from the tryptic peptide databases of N-Rne-wt and N-Rne-Q36R by adding the monoisotopic mass difference, m/z 242.2024 Da.

From extracted mass analysis of N-Rne-wt, we identified two peptides, [24]LYDLDIESPGHEQK[37] and [65]HGFLPLK[71], covalently linked to a uridine base of p-BR13. The [24]LYDLDIESPGHEQK[37] peptide includes the Q36 locus that is mutated in the hyperactive enzyme, while the [65]HGFLPLK[71] peptide contains the previously identified RNA contacting F67 amino acid residue of the S1 domain. We did not detect peptides linked to the other bases (cystidine, guanosine, and adenosine) of BR13, which is consistent with previous findings showing that uridine bases are preferentially UV crosslinked to RNA binding proteins.[30,31] The hyperactive enzyme peptide sequence corresponding to [24]LYDLDIESPGHEQK[37] (i.e., [24]LYDLDIESPGHER[36]) was not detected in the tryptic digests of this enzyme crosslinked by UV to pBR13 (**Fig. 8C**), suggesting that the Q36R mutation may interfere with UV crosslinking at this locus. The reduced crosslinking of the mutant protein, despite its higher binding affinity [5.8 and 3.2% of p-BR13 was crosslinked to N-Rne-wt and N-Rne-Q36R, respectively, when equimolar concentrations of p-BR13

phenylalanine, leucine, and cysteine) and the uridine base of RNA when both of the reacting groups lie within atomic distance.[30,31] The autoradiogram image showed that 5'-end-labeled p-BR13 was crosslinked to both the mutant and wild-type proteins (**Fig. 8A**).

Figure 7. Measurement of k_{cat} and K_m of N-Rne-wt and N-Rne-Q36R for cleavage of fluorogenic P-BR14-FD. Cleavage of various concentrations of P-BR14-FD (160 nM – 400 nM) by fixed concentration of N-Rne-wt and N-Rne-Q36R (10 nM) was monitored by fluorometry and measured data was transformed into a Lineweaver-Burk plot. Cleavage reaction was performed in cleavage buffer at 25°C.

The results of earlier experiments have suggested that RNase E can directly interact with substrates at two distinct sites, the 5' binding pocket and the S1 domain.[5,18,32,33] It has also been proposed that substrate RNA molecules containing a number of single stranded target sites within the substrate RNA can proceed directly with cleavage of substrate RNA, with the enzyme ignoring the phosphorylation status of the substrate (i.e., the "direct entry" model; see ref. 21). Our identification of an RNase E-derived uridine-bound peptide, [24]LYDLDIESPGHEQK[37], provides direct evidence that the region encompassing the Q36 site comes into close proximity with substrate RNA, and is likely to include a novel RNA binding site. However, if the novel contact point we have identified is used for direct entry of the enzyme onto substrates, enzyme molecules entering via this contact point must still be able, according to our data, to bind also at the 5' sensor site in order to distinguish between 5'-monophosphate and 5'-triphosphate termini. This requirement argues against a model in which some RNase E molecules bind to substrate RNA via the 5' sensor pocket, while others in the population bind via the contact point we have identified. As the crystallographically determined RNase E structure and the distance between the three contact points argues against the ability of the same enzyme molecule to bind concurrently to BR13 at the 5' pocket, the S1 domain, and the Q36 locus, we suggest a model in which use of the two binding sites is independent (**Fig. 9**). Paradoxically, the number of sites of RNA crosslinking decreased after the introduction of the Q36R mutation, but the mutation enhanced both the catalytic activity of the enzyme and its overall RNA binding as measured under EMSA conditions, which likely detects stable RNA-protein complexes that can survive migration through gel matrices. We suggest that the locus encompassing the Q36 site may facilitate transient formation of a 5' sensor-independent tether that serves as a *cis*-acting inhibitor of the enzyme's catalytic site (**Fig. 9A**). A local change in enzyme structure resulting from the Q36R mutation may enhance RNA binding at the primary binding site, contributing to the observed effect of the mutation on UV crosslinking of the catalytic region of the enzyme to p-BR13 (**Fig. 8A**) and on RNA binding affinities under protein saturation conditions (**Fig. 6**).

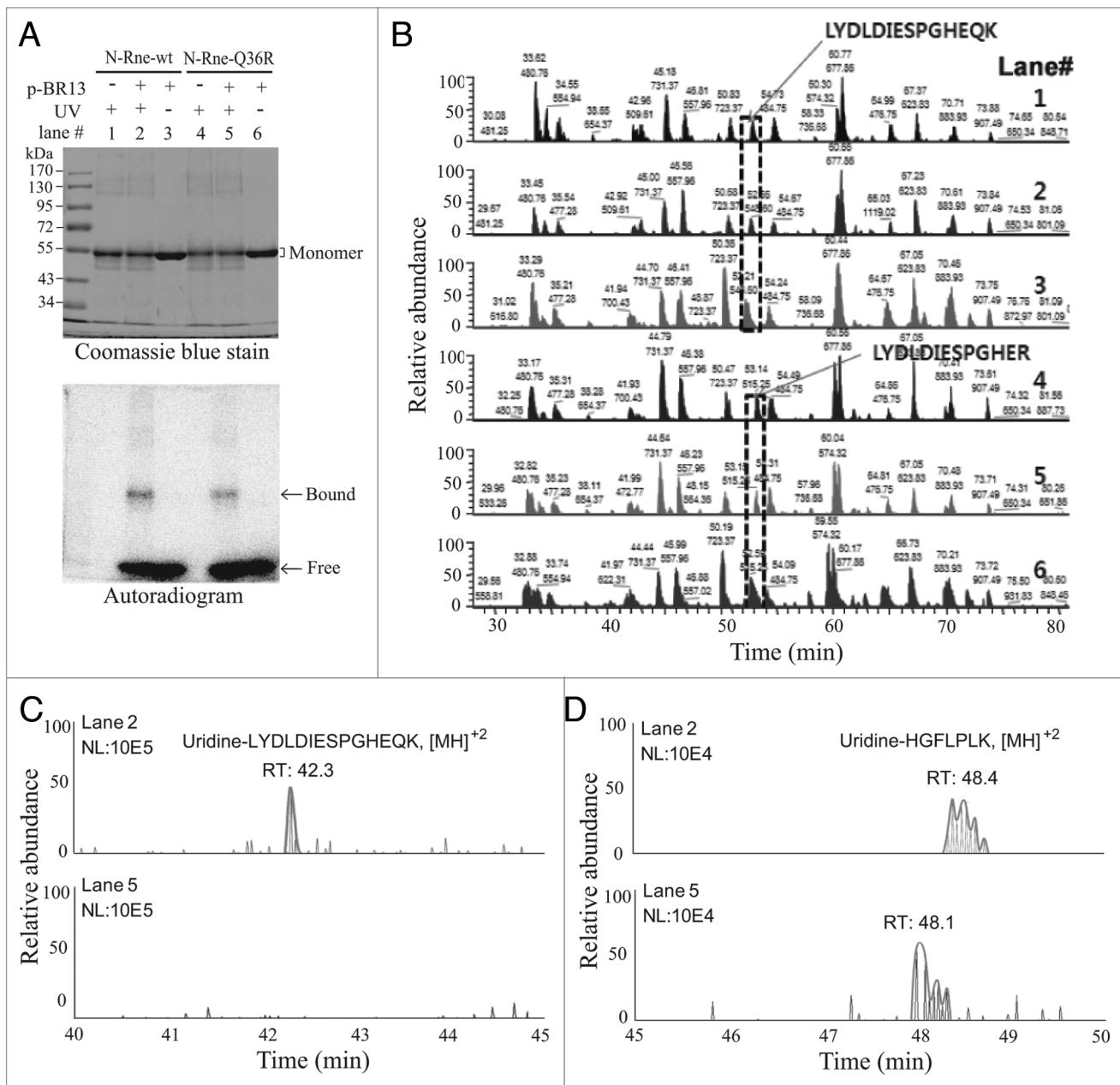and N-Rne proteins were used in the reactions (**Fig. 8A**)] is consistent with this interpretation.

Discussion

Our genetic screen for RNase E variants with enhanced ribonucleolytic activity identified a mutant that contains a single amino acid substitution (Q36R) that alters both the catalytic activity and binding properties of the enzyme. The fact that the viability of cells expressing the mutant protein can be maintained by reducing the level of expression of the mutant protein (**Fig. 1A**), and the decreased half-life of RNase E substrates in cells expressing it (**Fig. 2**), provide evidence of the overall physiological relevance of this mutant's effects.

The ability of the Q36R mutant protein to recognize and respond to the nature of the 5' terminus of substrates and to preferentially cleave substrates having 5'-monophosphate ends indicates that it retains the capacity characteristic of the wild-type enzyme to interact at its 5' sensor pocket with substrate RNA.[6] However, the ability of the Q36R mutation to increase binding to and cleavage of substrates having either type of terminus argues that the mutation affects an RNase E site that is functionally distinct from the 5' sensor pocket. The Q36R mutation is physically distinct from sites of interaction between enzyme and substrate that have been identified previously by X-ray analysis of the crystal structure of the N-terminal catalytic domain of *E. coli* RNase E in complex with various single-stranded oligonucleotide substrates, and is spatially distant from the 5' sensor as well as from the catalytic site and the S1 domain (**Fig. 1B**). Mass spectrometry analysis of enzyme fragments that were UV-crosslinked to RNA has suggested that the region of RNase E that encompasses the Q36 residue includes a previously unidentified RNA binding site of RNase E that is separate from the RNA-binding pocket that interacts with the 5' end of substrates and the S1 domain.

At least one other region that affects RNA binding and the rate of substrate cleavage by full length RNase E, but which is outside of the segment that has been studied by X-ray crystallography and also is not required for substrate specificity, has been identified.[1,7,34] The mechanism underlying the role of this region,

Figure 8. Analysis of N-Rne and p-BR13 complex. (A) UV crosslinking of N-Rne-wt and N-Rne-Q36R to p-BR13. (B) Mass chromatograms of tryptic peptides of N-Rne-wt and N-Rne-Q36R in the presence or absence of p-BR13 or UV irradiation. (C) Extracted mass spectra of uridine-bound 24LYDLDIESPGHEQK37 at m/z = 943.50 with the charge state of +2. (D) Extracted mass spectra of uridine-bound 65HGFLPLK71 at m/z = 527.34 with the charge state of +2. Log intensities of extracted mass spectra (expressed as 100%) are shown in the x-axes.

termed the arginine-rich RNA-binding domain (ARRBD; residues 592 to 684), in the actions of full length RNase E is also unknown.

Materials and Methods

Bacterial strains and plasmids. The strains and plasmids used in this study are listed in **Table 1**. Random mutations were introduced into the DNA fragment encoding amino acid residues 1-398 of RNase E using error-prone PCR,[22] and the PCR products were then digested with *Not*I and *Dra*III (NEB, #R0189S

and #R0510S) enzymes and ligated into sites of pNRNE4 generated by cleavage with these enzymes. The primers used were Nrne-5' (5'-GAATTGTGAGCGGATAAC-3') and Nrne-3' (5'-CTACCATCGGCGCTACGT-3'). Plasmid pLAC-RNE2-Q36R was constructed by subcloning the *Not*I and *Pml*I (NEB, #R0532S) fragment of pNRNE4-Q36R into the same restriction enzyme sites in pLAC-RNE2. Site-directed mutagenesis and overlap extension PCR were carried out to construct pNRNE4-Q36A. Two DNA fragments were synthesized using primers Nrne 5', Rne-Q36A-R (5'-CGCCTCGTGCCCTGGACTTTC-3'), Rne-Q36A-F (5'GGC ACG AGG CGA AAA AGG
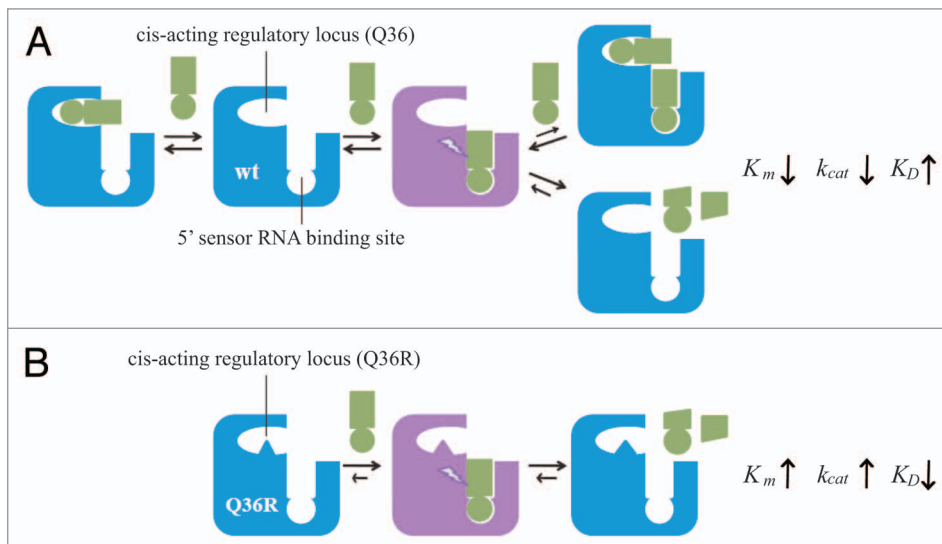
Figure 9. A model for the functional role of the *cis*-acting regulatory locus of RNase E. Catalytically active and inactive forms of N-Rne-wt and N-Rne-Q36R are shown, violet and blue, respectively. RNA is shown in green. The size of arrows indicates relative reaction rates, which were hypothesized by assuming that EMSAs detected the complex of RNA and catalytically active forms of N-Rne-wt and N-Rne-Q36R. (A) Representation of the model of wild-type enzyme activity. The *cis*-acting regulatory locus (Q36) facilitates the transient formation of a 5′ sensor-independent tether between the RNA and protein that inhibits interaction between the RNA and the enzyme's catalytic site. (B) Representation of the model of Q36R mutant enzyme activity. The Q36R mutation interferes with the ability of the Q36 locus to bind substrate, leading to a loss of enzymatic inhibition.

CAA ACA TCT ACA AA-3') and Rne-561R (5'-AGT CCA GGG CAC GAG GCG AAA AAG GCA AAC ATC TAC AAA-3'). Synthetic DNA fragments were combined using primers Nrne-5' and Rne-561R. The PCR products were then digested with *Not*I and *Hin*dIII (NEB, #R0104S) enzymes and ligated into sites of pNRNE4 generated by cleavage with these enzymes.

Northern blot analysis. Northern blot analysis was performed as described previously.[23] DNA oligonucleotides used for probing RNA I transcripts synthesized from pNRNE4 and *rpsT* mRNA were RNA I-A (5'-GAG CTA CCA ACT CTT TGA ACC

GA-3') and rpsT (5'-GTC CAA CTC CCA AAT GTG TTC-3'), respectively.

Western blotting and circular dichroism (CD) analyses. Procedures for western blot analyses of Rne, N-Rne, and S1 have been previously described.[23] N-Rne-wt and N-Rne-Q36R proteins were purified from KSL2000 cells harboring pNRNE4 and pNRNE4-Q36R, respectively, as described previously.[23] For circular dichroism analysis, purified proteins were dialyzed in CD buffer (20 mM NaH_2PO_4, pH 7.5 and 200 mM NaCl). Spectra were collected in the range of 200-280 nm at intervals of 1 nm, with three accumulations being recorded on a JASCO J-715 spectropolarimeter. Spectra were measured at a protein concentration of 0.2 mg/ml in a 0.1 cm cell.

In vitro cleavage of RNase E substrates. Synthesis of 5'-end-labeled BR13 (p-BR13) and BR30 (p-BR30), and uniformly labeled p23 RNA was performed as described previously.[23] Uniformly labeled 5'-triphosphorylated BR13 (ppp-BR13) with [α-32P]-UTP was synthesized from synthetic oligonucleotides containing the sequence of the T7 promoter followed by the sequence of BR13 using the MEGAshortscript™ T7 kit (Applied Biosystems, #AM1354) according to the manufacturer's instruction. Forty-five micrometers of oligonucleotides, T7-BR13-5' (5'- TAA TAC GAC TCA CTA TAG GGA CAG TAT TTG-3') and T7-BR13-3' (5'-CAA ATA CTG TCC CTA TAG TGA GTC GTA TTA-3'), were mixed in an annealing buffer (20 mM Tris-Cl pH 8.0, 1.5 mM NaCl, and 100 mM EDTA), incubated at 95°C for 2 min, and

Table 1. *E. coli* strains and plasmids used in this study

Strain/Plasmid	Description	Reference
N3433	*lacZ43*(Fs) LAM- *relA1 spoT1 thi-1*	40
KSL2000	Same as N3433 but *rne::cat recA::Tn10* [pBAD-RNE]	23
KSL2003	Same as N3433 but *rne::cat recA::Tn10* [pLAC-RNE2]	23
KSL2003-Q36R	Same as KSL2003 but [pLAC-RNE2-Q36R]	This study
pACYC177	p15A *ori*, Ap^r, Km^r	41
pBAD-RNE	pSC101 *ori*, Km^r, *rne* under PBAD	23
pET28a	pMB1 *ori*, Km^r	Novagen
pLAC-RNE2	pSC101 *ori*, Ap^r, *rne* under PlacUV5	23
pLAC-RNE2-Q36R	pSC101 *ori*, Ap^r, *rne* -Q36R under PlacUV5	This study
pNRNE4	p15A *ori*, Ap^r, *N-rne* under PlacUV5	24
pNRNE4-Q36R	p15A *ori*, Ap^r, *N-rne*-Q36R under PlacUV5	This study
pNRNE4-Q36A	p15A *ori*, Ap^r, *N-rne*-Q36A under PlacUV5	This study
pNRNE4-V236E	p15A *ori*, Ap^r, *N-rne*-V236E under PlacUV5	This study

cooled down slowly to ~20°C for ~1 hr. Synthesized ppp-BR13 transcripts were purified from a 15% polyacrylamide gel containing 8 M urea. RNase E cleavage assays were performed as described previously.[35]

Kinetic characterization of cleavage activity of N-Rne and N-Rne-Q36R. Cleavage of fluorogenic oligonucleotide P-BR14-FD[9] was monitored by fluorometry using a Tecan i-control Infinite R 200 pro microplate reader (exitation at 485 nm and emission at 535 nm). The cleavage assay was performed in cleavage buffer at 25°C with various concentrations of P-BR14-FD (160 nM–400 nM) and a fixed concentration of N-Rne-wt and N-Rne-Q36R (10 nM).

Electrophoretic mobility shift assay (EMSA). Approximately one pmol of 5'-end labeled BR13 (p-BR13), or uniformly labeled BR13 (ppp-BR13), RNA I or p23 RNA was incubated with increasing concentrations of N-Rne-wt or N-Rne-Q36R for 5 min at 4°C in 100 μl of a buffer containing 10 mM Tris-HCl, pH 7.5, 0.1 mM DTT, 1 mM EDTA and 10% (v/v) glycerol. The reaction products were loaded on to an 8% TBE native gel (1x TBE, 8% acrylamide/bis solution (19:1), 2.5% glycerol) and separated.

UV crosslinking. To crosslink the subunits of N-Rne-wt and N-Rne-Q36R, 40 pmol of purified proteins in 40 μl of a buffer containing 75 mM Tris-HCl, pH 7.5, 750 mM NaCl, 1.5 mM EDTA, and 1.5 mM DTT were exposed to UV light (254 nm) in a CL1000 Ultraviolet Cross Linker (UVP). Samples were removed at different time intervals, mixed with an equal volume of protein loading buffer (100 mM Tris-Cl pH 6.8, 4% SDS, 0.2% bromophenol blue, 30% glycerol, and 200 mM β-mercaptoethanol), and separated by 10% SDS-PAGE. To crosslink N-Rne proteins with p-BR13 RNA, 20 pmol of 5'-end labeled BR13 (p-BR13) was incubated with 20 pmol of N-Rne-wt or N-Rne-Q36R in 40 μl of the buffer used in EMSA at 4°C for 5 min, and the reaction mixtures were irradiated by UV light for 30 min. The autoradiogram of RNA-protein complexes induced by UV crosslinking was examined by separation on 10% SDS-PAGE gels including experimental controls without addition of p-BR13, or without UV irradiation.

LC-MS/MS experiments. Coomassie blue-stained protein bands were excised from two gels, and destained gel slices were treated twice with 50 mM NaOH at 60°C for 15 min on an Eppendorf Thermomixer in order to cleave phospho-diester bonds in RNA. Tryptic peptides were prepared by the in-gel digestion method,[36] and analyzed using a nanoACQUITY UPLC (NanoA, Waters) system. After the preparation of tryptic peptides, phosphate removal from RNA-protein complex obtained from one gel was examined using Titansphere Phos-TiO kits (GL Sciences, 5010-21300) according to the phospho enrichment method. The LC system was equipped with an RPLC column (75 μm inner diameter × 360 μm outer diameter × 75 cm length) which was packed in house with C18 particles (3 μm, 300 Å pore size, Jupiter, Phenomenex)[37] and an SPE column which was

manufactured by packing a 1 cm-long liner (250-μm inner diameter) inside of an internal reducer (1/16 to 1/32 in; VICI) with the same C18-bonded particles. The tryptic peptides were loaded onto the online SPE column for 3 min with solvent A (0.1% formic acid in water) and eluted from the capillary column with a 120-min linear gradient of 10–60% solvent B (0.1% formic acid in acetonitrile) at a flow rate of 0.40 μl/ min.

A 7-T Fourier transform ion cyclotron resonance mass spectrometer (LTQ-FT, Thermo Electron) was used to collect the mass spectra. To reduce background noises, MS precursor ion scans (*m/z* 450-2000) were acquired in a profile mode with an automated gain control (AGC) target value of 1.0×10^6, a mass resolution of 1.0×10^5, and a maximum ion accumulation time of 1000 ms. The mass spectrometer was operated in a data-dependent tandem MS mode where a full-scan MS experiment was followed by MS/MS experiments on the seven most abundant ions in the precursor MS scan. Normalized collision energy of 35% was used for precursor fragmentation with isolation width of 3 THz. A dynamic exclusion option (exclusion mass width low, 1.10 THz; exclusion mass width high, 2.10 THz; exclusion list size, 120; exclusion duration, 30 s) was incorporated to prevent reacquisition of MS/MS spectra of the same peptides. LC/MS/MS data were subjected to the integrated post-experiment monoisotopic mass refinement (*i*PE-MMR) process to increase the accuracy of precursor masses of tandem mass spectra before protein database search, as described in details elsewhere.[38,39]

The resultant MS/MS data were subjected to search against a database containing N-Rne sequence and N-Rne-Q36R mutation in a common contaminant database using SORCERER-SEQUEST™ (Version 27, Revision 12, Sage-N Research, Inc.). Extracted mass chromatograms were manipulated using Qual Browser version 2.0.7 (Thermo Fisher Scientific). The database search was performed using a precursor mass tolerance of 10 ppm and a fragment mass tolerance of 1 Da with the modification options of static carbamidomethylation (+57.021460 Da) at cysteine, or variable uridine (+242.2024 Da) at methionine, tyrosine, histidine, phenylalanine, leucine, or cysteine.

Note

Supplemental materials can be found at:
www.landesbioscience.com/journals/rnabiology/article/18063

References

1. McDowall KJ, Cohen SN. The N-terminal domain of the rne gene product has RNase E activity and is non-overlapping with the arginine-rich RNA-binding site. J Mol Biol 1996; 255:349-55;PMID;10.1006/jmbi.1996.0027.

2. Kido M, Yamanaka K, Mitani T, Niki H, Ogura T, Hiraga S. RNase E polypeptides lacking a carboxyl-terminal half suppress a *mukB* mutation in *Escherichia coli*. J Bacteriol 1996; 178:3917-25.

3. Ow MC, Liu Q, Kushner SR. Analysis of mRNA decay and rRNA processing in *Escherichia coli* in the absence of RNase E-based degradosome assembly. Mol Microbiol 2000; 38:854-66.

4. Caruthers JM, Feng Y, McKay DB, Cohen SN. Retention of core catalytic functions by a conserved minimal ribonuclease E peptide that lacks the domain required for tetramer formation. J Biol Chem 2006; 281:27046-51.

5. Callaghan AJ, Marcaida MJ, Stead JA, McDowall KJ, Scott WG, Luisi BF. Structure of *Escherichia coli* RNase E catalytic domain and implications for RNA turnover. Nature 2005; 437:1187-91.

6. Garrey SM, Blech M, Riffell JL, Hankins JS, Stickney LM, Diver M et al. Substrate binding and active site residues in RNases E and G: role of the 5'-sensor. J Biol Chem 2009; 284:31843-50;PMID;10.1074/jbc.M109.063263.

7. Taraseviciene L, Bjork GR, Uhlin BE. Evidence for an RNA binding region in the *Escherichia coli* processing endoribonuclease RNase E. J Biol Chem 1995; 270:26391-8.

8. Carpousis AJ. The RNA degradosome of *Escherichia coli*: an mRNA-degrading machine assembled on RNase E. Annu Rev Microbiol 2007; 61:71-87.

9. Jiang X, Belasco JG. Catalytic activation of multimeric RNase E and RNase G by 5'-monophosphorylated RNA. Proc Natl Acad Sci USA 2004; 101:9211-6.

10. Callaghan AJ, Redko Y, Murphy LM, Grossmann JG, Yates D, Garman E et al. "Zn-link": a metal-sharing interface that organizes the quaternary structure and catalytic site of the endoribonuclease, RNase E. Biochemistry 2005; 44:4667-75.

11. Taghbalout A, Rothfield L. RNaseE and the other constituents of the RNA degradosome are components of the bacterial cytoskeleton. Proc Natl Acad Sci USA 2007; 104:1667-72.

12. Casarégola S, Jacq A, Laoudj D, McGurk G, Margarson S, Tempete M et al. Cloning and analysis of the entire *Escherichia coli* ams gene. *ams* is identical to *hmp1* and encodes a 114kDa protein that migrates as a 180 kDa protein. J Mol Biol 1992; 228:30-40.

13. Coburn GA, Mackie GA. Degradation of mRNA in *Escherichia coli*: an old problem with some new twists. Prog Nucleic Acid Res Mol Biol 1999; 62:55-108.

14. Steege DA. Emerging features of mRNA decay in bacteria. RNA 2000; 6:1079-90.

15. Carpousis AJ, Luisi BF, McDowall KJ. Endonucleolytic initiation of mRNA decay in *Escherichia coli*. Prog Mol Biol Transl Sci 2009; 85:91-135.

16. Mackie GA. Ribonuclease E is a 5'-end-dependent endonuclease. Nature 1998; 395:720-4.

17. Feng Y, Vickers TA, Cohen SN. The catalytic domain of RNase E shows inherent 3' to 5' directionality in cleavage site selection. Proc Natl Acad Sci USA 2002; 99:14746-51.

18. Koslover DJ, Callaghan AJ, Marcaida MJ, Garman EF, Martick M, Scott WG et al. The crystal structure of the *Escherichia coli* RNase E apoprotein and a mechanism for RNA degradation. Structure 2008; 16:1238-44.

19. Deana A, Celesnik H, Belasco JG. The bacterial enzyme RppH triggers messenger RNA degradation by 5' pyrophosphate removal. Nature 2008; 451:355-8.

20. Celesnik H, Deana A, Belasco JG. Initiation of RNA decay in *Escherichia coli* by 5' pyrophosphate removal. Mol Cell 2007; 27:79-90.

21. Kime L, Jourdan SS, Stead JA, Hidalgo-Sastre A, McDowall KJ. Rapid cleavage of RNA by RNase E in the absence of 5'-monophosphate stimulation. Mol Microbiol 2009; 76:590-604.

22. Shin E, Go H, Yeom JH, Won M, Bae J, Han SH, et al. Identification of amino acid residues in the catalytic domain of RNase E essential for survival of *Escherichia coli*: functional analysis of DNase I subdomain. Genetics 2008; 179:1871-9.

23. Lee K, Bernstein JA, Cohen SN. RNase G complementation of *rne* null mutation identifies functional interrelationships with RNase E in *Escherichia coli*. Mol Microbiol 2002; 43:1445-56.

24. Tamura M, Lee K, Miller CA, Moore CJ, Shirako Y, Kobayashi M et al. RNase E maintenance of proper FtsZ/FtsA ratio required for nonfilamentous growth of *Escherichia coli* cells but not for colony-forming ability. J Bacteriol 2006; 188:5145-52.

25. Lin-Chao S, Wong TT, McDowall KJ, Cohen SN. Effects of nucleotide sequence on the specificity of *rne*-dependent and RNase E-mediated cleavages of RNA I encoded by the pBR322 plasmid. J Biol Chem 1994; 269:10797-803.

26. Lee K, Cohen SN. A *Streptomyces coelicolor* functional orthologue of *Escherichia coli* RNase E shows shuffling of catalytic and PNPase-binding domains. Mol Microbiol 2003; 48:349-60.

27. Yeom J-H, Lee K. RraA rescues *Escherichia coli* cells over-producing RNase E from growth arrest by modulating the ribonucleolytic activity. Biochem Biophys Res Commun 2006; 345:1372-6.

28. Rapaport LR, Mackie GA. Influence of translational efficiency on the stability of the mRNA for ribosomal protein S20 in *Escherichia coli*. J Bacteriol 1994; 176:992-8.

29. Kim S, Kim H, Park I, Lee Y. Mutational analysis of RNA structures and sequences postulated to affect 3' processing of M1 RNA, the RNA component of *Escherichia coli* RNase P. J Biol Chem 1996; 271:19330-7.

30. Shetlar MD. Cross-linking of proteins to nucleic acids by ultraviolet light. Photochem Photobiol Rev 1980; 5:105-97.

31. Urlaub H, Kuhn-Holsken E, Luhrmann R. Analyzing RNA-protein crosslinking sites in unlabeled ribonucleoprotein complexes by mass spectrometry. Methods Mol Biol 2008; 488:221-45;PMID;10.1007/978-1-60327-475-3_16.

32. Baker KE, Mackie GA. Ectopic RNase E sites promote bypass of 5'-end-dependent mRNA decay in *Escherichia coli*. Mol Microbiol 2003; 47:75-88.

33. Hansen MJ, Chen LH, Fejzo ML, Belasco JG. The *ompA* 5' untranslated region impedes a major pathway for mRNA degradation in *Escherichia coli*. Mol Microbiol 1994; 12:707-16.

34. Kaberdin VR, Walsh AP, Jakobsen T, McDowall KJ, von Gabain A. Enhanced cleavage of RNA mediated by an interaction between substrates and the arginine-rich domain of *E. coli* ribonuclease E. J Mol Biol 2000; 301:257-64;PMID;10.1006/jmbi.2000.3962.

35. McDowall KJ, Kaberdin VR, Wu SW, Cohen SN, Lin-Chao S. Site-specific RNase E cleavage of oligonucleotides and inhibition by stem-loops. Nature 1995; 374:287-90.

36. Kim HJ, Kang HJ, Lee H, Lee ST, Yu MH, Kim H et al. Identification of S100A8 and S100A9 as serological markers for colorectal cancer. J Proteome Res 2009; 8:1368-79.

37. Keller A, Nesvizhskii AI, Kolker E, Aebersold R. Empirical statistical model to estimate the accuracy of peptide identifications made by MS/MS and database search. Anal Chem 2002; 74:5383-92.

38. Jung HJ, Purvine SO, Kim H, Petyuk VA, Hyung SW, Monroe ME et al. Integrated Post-Experiment Monoisotopic Mass Refinement: An Integrated Approach to Accurately Assign Monoisotopic Precursor Masses to Tandem Mass Spectrometric Data. Anal Chem 2010; 82:8510-8.

39. Shin B, Jung HJ, Hyung SW, Kim H, Lee D, Lee C et al. Postexperiment monoisotopic mass filtering and refinement (PE-MMR) of tandem mass spectrometric data increases accuracy of peptide identification in LC/MS/MS. Mol Cell Proteomics 2008; 7:1124-34.

40. Goldblum K, Apirion D. Inactivation of the ribonucleic acid-processing enzyme ribonuclease E blocks cell division. J Bacteriol 1981; 146:128-32.

41. Chang AC, Cohen SN. Construction and characterization of amplifiable multicopy DNA cloning vehicles derived from the P15A cryptic miniplasmid. J Bacteriol 1978; 134:1141-56.

42. Perez-Iratxeta C, Andrade-Navarro MA. K2D2: estimation of protein secondary structure from circular dichroism spectra. BMC Struct Biol 2008; 13:8-25.